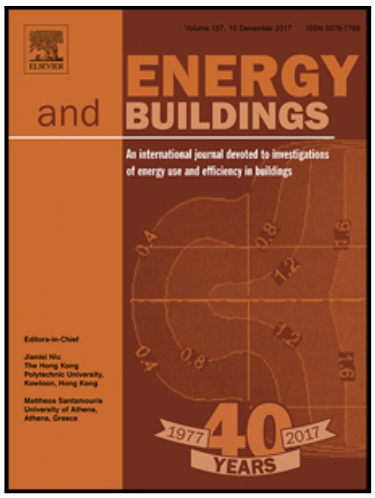

Integrated hollow porous ceramic cuboids-finned heat pipes evaporative cooling system: numerical modelling and experimental validation

Abdulrahman Alharbi , Abdulmajeed Almaneea , Rabah Boukhanouf

PII: S0378-7788(18)31881-4
DOI: https://doi.org/10.1016/j.enbuild.2019.05.012
Reference: ENB 9173

To appear in: *Energy & Buildings*

Received date: 29 July 2018
Revised date: 3 April 2019
Accepted date: 4 May 2019

Please cite this article as: Abdulrahman Alharbi , Abdulmajeed Almaneea , Rabah Boukhanouf , Integrated hollow porous ceramic cuboids-finned heat pipes evaporative cooling system: numerical modelling and experimental validation, *Energy & Buildings* (2019), doi: https://doi.org/10.1016/j.enbuild.2019.05.012

Highlights

- Investigation of novel hollow porous ceramic cuboids-heat pipes as heat and mass exchanger for evaporative cooling systems
- Formulation of mathematical model for heat and mass transfer
- Testing a proof-of-concept laboratory model

Title: *Integrated hollow porous ceramic cuboids-finned heat pipes evaporative cooling system: numerical modelling and experimental validation*

Authors: Abdulrahman Alharbi [a], Abdulmajeed Almaneea* [b], Rabah Boukhanouf [c]

Affiliations:

[a] General presidency for the affairs of holy mosque and the prophet's mosque, Makkah, Kingdom of Saudi Arabia.

[b] Department of Mechanical Engineering , College of Engineering , Majmaah University, Majmaah 11952, Kingdom of Saudi Arabia.

[c] The University of Nottingham, Department of Architecture and Built Environment, Faculty of Engineering, Nottingham NG7 2RD, United Kingdom.

Contact email: *a.almaneea@mu.edu.sa

Abstract

The work presented in this paper investigates design, computer modelling and testing of a sub-wet bulb temperature evaporative cooling system for space air conditioning in buildings. The target application of evaporative cooling technology is particularly for geographical regions with hot and dry climate. A laboratory prototype made of integrated finned heat pipes and a water filled hollow porous ceramic cuboids was been built and tested. The design exploits the high thermal conductivity of heat pipes as effective heat transfer device and the good wettability characteristic of porous ceramic material. Key thermal performance metrics of the prototype were modelled and validated experimentally under controlled laboratory conditions of temperature (30, 35 and 40 ^{o}C) and relative humidity (35 to 55%). Under typical dry climates conditions (ambient air dry bulb temperature of 35^{o}C and relative humidity of 35%), the measured supply air dry bulb temperature was 22.3 ^{o}C, which is lower that the ambient air wet bulb temperature, and maximum cooling capacity of approximately 196 W per unit surface area (m^{2}) of wet porous ceramic cuboid. Furthermore, it was shown that the measured prototype cooler wet bulb effectiveness was 1.05 while the dew point effectiveness was 0.73.

Nomenclature

Symbol	description	Unit
A	*Heat and mass transfer area*	*(m^2)*
A_f	*The finned section heat transfer area*	*(m^2)*
A_{dh}	*Hydraulic diameter of rectangular ducts*	*(m^2)*
C_c	*Cost of electricity consumption*	*(SAR/kWh)*
C_p	*Specific heat of humid air*	*(J kg^{-1} K^{-1})*
C_{pfw}	*Specific heat of water*	*(J kg^{-1} K^{-1})*
E_c	*The power consumption*	*(kWh)*
g_a	*Air moisture content in wet channel*	*(kg water/ kg dry air)*
g_d	*Air moisture content in dry channel*	*(kg water/ kg dry air)*
g_{fw}	*Saturated air moisture content*	*(kg water/ kg dry air)*
h	*Specific enthalpy*	*(J/kg)*
h_{fg}	*Latent heat of vaporization of water*	*(kJ/kg)*
K_s	*Overall heat transfer coefficient*	*($Wm^{-2}K^{-1}$)*
l_1	*Length of the wick*	*(m)*
Le	*Lewis number*	
m	*Depends on the fin properties*	
m_a	*Air mass flow rate dry channel*	*(kg/s)*
m_d	*Air mass flow rate wet channel*	*(kg/s)*
m_s	*Supply mass flow rate ($m_d - m_a$)*	*(kg/s)*
Nu	*Nusselt number*	
q_c	*Specific cooling capacity*	*(W/m^2)*
r_1	*Inner of the wick*	*(m)*
r_2	*Outer of the wick*	*(m)*
R_{ao}	*Thermal resistance of the wet channel*	*(W/m^2)*
R_{cp}	*Thermal resistance of the saturated ceramic*	*(K/W)*
R_{di}	*Thermal resistance of the dry channel*	*(K/W)*
R_{me}	*Thermal resistance of the heat pipe wick of the*	*(K/W)*
R_w	*Thermal resistance of the water in the ceramic*	*(K/W)*
t	*Thickness*	*(m)*
t_a	*Wet channel air temperature*	*(^oC)*
T_d	*Dry channel air temperature*	*(^oC)*

T_{fw}	*Water film temperature*	*(^oC)*
T_{wb}	*Wet bulb temperature*	*(^oC)*
$\dot{V}$	*Air flow rate*	*(m^3/s)*
ρ	*Air density*	*(kg/m^3)*
α	*Convective heat transfer coefficient*	*($W/(m^2 K)$)*
σ	*Mass transfer coefficient*	*($kg_{water}/s\ m^2)/kg_{dry}$)*
δ_f	*Fins thickness*	*(m)*
λ_1	*Thermal conductivity of the liquid phase of the*	*(W/mK)*
λ_c	*Thermal conductivity of the dry ceramic container*	*(W/mK)*
λ_f	*Fins thermal conductivity*	*(W/mK)*
λ_s	*Thermal conductivity of heat pipe wick material*	*(W/mK)*
λ_w	*Water thermal conductivity*	*(W/mK)*
λ_{wick}	*Thermal conductivity of the wick*	*(W/mK)*
ϕ_c	*Ceramic container porosity*	*(%)*
ϕ_{wick}	*Wick porosity*	*(%)*
η_f	*Efficiency of the finned section heat exchanger*	
ε_{wb}	*Wet bulb effectiveness*	
ε_{dp}	*Dew point effectiveness*	
Subscript	*description*	
a	*Wet channel*	
d	*Dry channel*	
i	*Inlet*	
o	*Outlet*	
w	*Water*	
fw	*Film of water*	
wb	*Wet bulb temperature*	
dp	*Dry bulb temperature*	

1. Introduction

It is well known that the building sector consumes over 40% of global energy resources [1, 2]. A major share of the energy is used for space heating and cooling to provide thermal comfort for buildings' occupants. In parts of the world with unfavourable hot climates, a high demand for packaged mechanical air conditioning systems has increased households electricity consumption. Therefore, alternative low energy systems and processes are needed more than ever to address the escalation of power demand and climate change issues. Evaporative cooling lends itself well for cooling and humidification applications for buildings in hot, arid climates at a fraction of the energy consumption compared to other energy intensive mechanical systems such as vapour compression air conditioning systems.

The concept of evaporative cooling is well understood. In its simplest forms, evaporative cooling consists of a simple wet fabric or textile placed over a building opening such as a door or window frame in the summer to allow a breeze of cool air to trickle into the building's living space [3]. Today, evaporative cooling systems use advanced designs and materials for adaption for modern building [4]. For example, in Saudi Arabia, there are over 48,000 rooftop-mounted direct evaporative air coolers installed in temporary tents accommodation, places of worship, railway stations and public spaces [5].

Evaporative cooling systems can be classified into two main categories: direct and indirect coolers. Direct evaporative cooling (DEC) is a passive air cooling process in which exposure of a water surface to surrounding air causes a drop of the air dry bulb temperature and an increase of its latent heat and moisture content. In modern DEC systems, water and air are brought into contact in a wet media core (pad) which is made of cellulose or organic material with large air-water contact surface. The thermal performance of such systems is strongly affected by the design and characteristics of the pad and prevailing climatic conditions [6, 7]. In contrast, an indirect evaporative cooler (IEC) supplies cool air without increasing its moisture content. This is accomplished by arranging air channels in parallel to form alternate wet and dry air passages. The channels are made of waterproof thin plates with the wet channel inner walls lined up with a wet material for water retention. The two airflows in the dry and wet channel exchange heat through the thin plate wall channel cooling the supply air indirectly and without increasing its moisture while the airflow in the wet channel is rejected saturated at near its wet bulb conditions, as shown in Fig. 1.

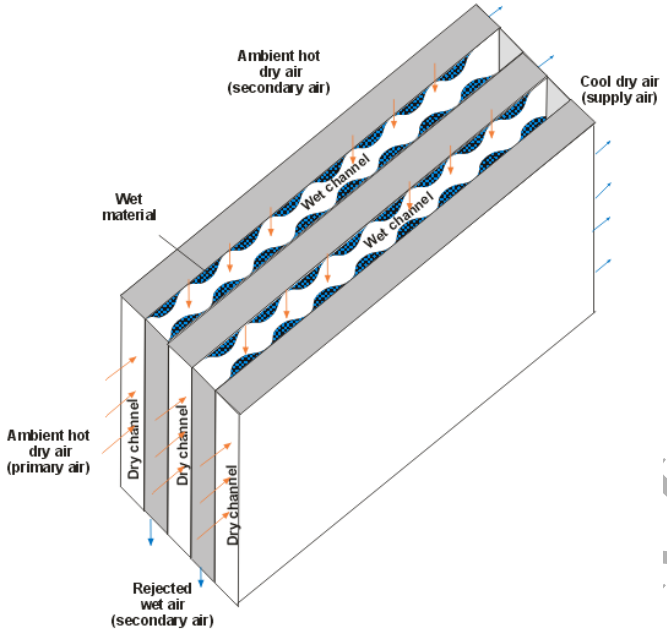

Fig. 1. *Simplified schematic of IEC*

In addition to suffering similar limitations of DEC, the performance of IEC is further compounded by heat transfer irreversibilities, leading to reduced potential to cooling supply air to only 2-3 ^{o}C above the wet bulb temperature. This constitutes a severe disadvantage compared to vapour mechanical air-conditioning systems, which are less prone to changes of ambient air conditions. A design variant of IEC systems capable of cooling ambient air below its wet bulb temperature is known as dew point or sub wet bulb temperature evaporative cooling [8]. This is achieved by redirecting part of the dry, cool supply air of the dry channel through the wet channel, as shown in Fig. 2.

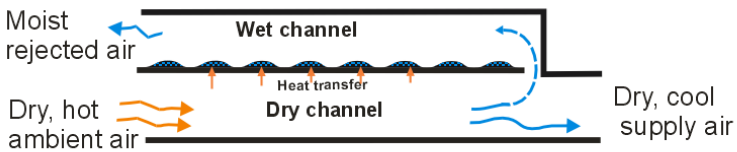

Fig. 2. *Simplified schematic of Dew Point DPEC*

The development of sub wet bulb temperature evaporative cooling systems have been the subject of many publications by leading researchers [9, 10, 11]. Most of these investigations focused on improving

the design of the compact heat and mass exchanger (HMX), which is usually constructed form edge-welded thin sheets to provide multi flow paths (cross flow and counterflow) for the air in the dry and wet channels. Other design improvements of evaporative cooling systems include using heat pipes as heat transfer devices and porous ceramic materials as wet media materials. For example, Ibrahim et al. [12] used water filled ceramic containers to form a direct evaporative cool wall. Similarly, Chen et al. [13] used porous ceramic pipes with high water sucking ability in a direct evaporative cooling wall. The passive evaporative cooling wall was constructed of three rows of porous ceramic pipes placed vertically in a staggered or parallel array arrangement, as shown in Fig. 3. The authors found that the porous ceramic pipe surface temperature was 4 –6 ^{o}C below the ambient while the airflow through the wall was cooled by 3 - 5 ^{o}C.

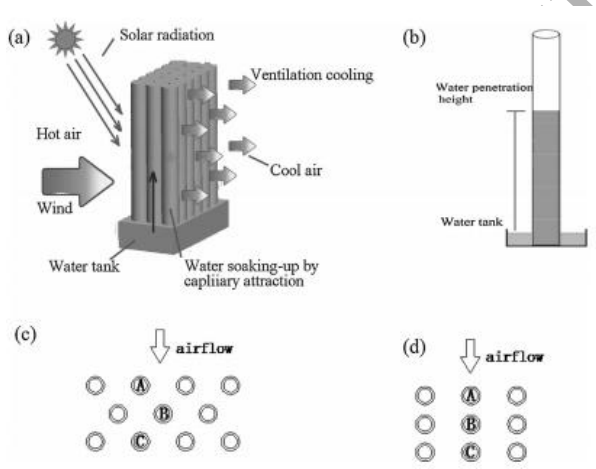

Fig. 3. *Schematic of passive evaporative cooling wall constructed of porous ceramic pipes with water soaking-up ability, (a) Cooling wall, (b) Single porous ceramic pipe and water tank, (c) Porous ceramic pipes in staggered-array arrangement, (d) Porous ceramic pipes in parallel arrangement*

Wang et al. [14] investigated the design and modelling of a novel porous ceramic tube indirect evaporative cooler (IEC) to improve the surface hydrophilicity in the wet channels. The authors tested a laboratory prototype under various operating conditions, as shown in Fig. 4. It was reported that using a porous ceramic material improved water retention and reduced energy consumption of the water-spraying pump. However, the system achieved a modest wet-bulb effectiveness of about 42%.

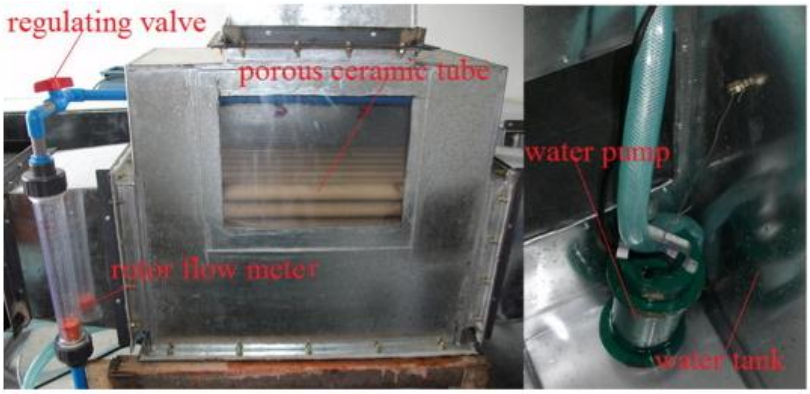

Fig. 4. *Laboratory set up of porous ceramics tube type IEC.*

Riffat and Zhu [15] developed an IEC system that integrates heat pipes and porous ceramic cuboids. The porous ceramic cuboids form part of the wet channel while the heat pipes were used to transfer heat from the air in the dry channel to the air in the wet channel. The mathematical model developed by the authors shows that the thermal conductivity between the heat pipe and the ceramic cooler was improved to achieve better performance. Boukhanouf et al. [16] developed a sub wet bulb temperature evaporative cooler using cylindrical porous ceramic tube fitted as sleeves over the condenser of the heat pipe. The authors showed the system could provide adequate thermal comfort for buildings even under sever climate conditions.

2. Research Context

Many researchers investigated various design configurations, thermal performance indices and applications of evaporative cooling systems. In addition, recent advancements of evaporative cooling design have centred on instigating the use of new materials with suitable properties (e.g., hydrophilicity, wettability, thermal conductivity, etc.) and mechanical configurations that can augment heat and mass transfer in DEC and IEC systems. Nevertheless, there is still a need for in-depth research on theoretical and experimental aspects of novel evaporative cooling technology and associated heat and mass transfer mechanisms. For instance, current state of the art sub wet bulb temperature coolers have been fitted with a densely packed HMX that requires critical manufacturing quality assurance to minimise air leakage, contamination and *fan-power. This work attempts to advance the design of sub-wet bulb temperature evaporative cooling system by using rigid modular HMX core made of porous ceramic materials as wet media and finned heat pipes as effective devices for heat and mass transfer. This presents inherent advantages for integration with a building envelope. The scope of the research*

methodology includes formulating a mathematical model, designing the experiment and testing a prototype under controlled laboratory conditions, as summarised in the flow diagram of Fig. 5. The different stages of the research have been described in details including the formulation of the computer model, design of the experiment and analysis of the results of theoretical and experimental performance of the system.

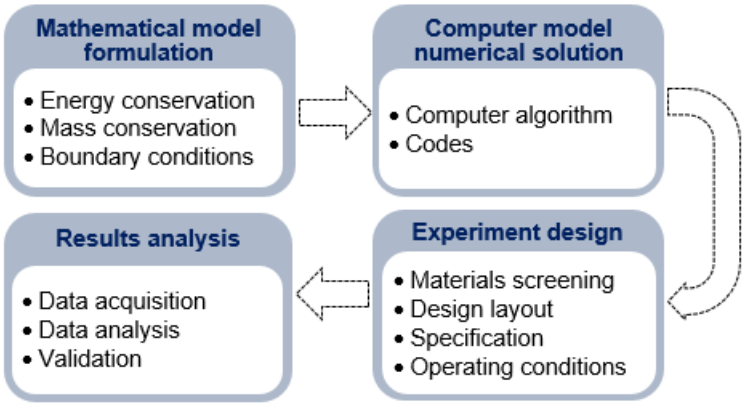

Fig. 5. *Steps of the research design*

3. Methodology

3.1 Description of the system

A simplified mechanical arrangement of the Dew Point (DP) indirect evaporative cooler considered in this study is shown in Fig. 6. The heat and mass exchanger (HMX) core module is made of finned heat pipes and porous ceramic cuboid and is housed in an outer casing to form the dry and wet air channels. The heat pipes are of tubular shape with finned evaporator section, which transfer heat from the hot, dry air in the dry channel to the condenser section that is inserted in the water-filled porous ceramic cuboid in the wet channel. Narrow air ducts were formed around the porous ceramic-heat pipe modules using Perspex sheets.

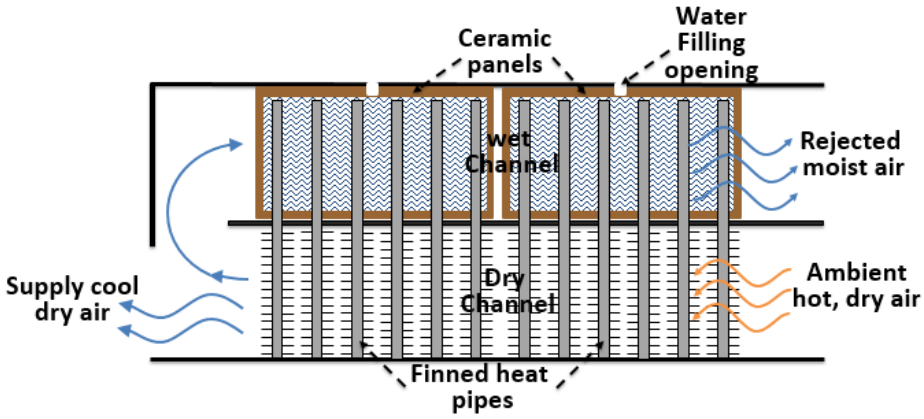

Fig. 6. *A schematic of heat pipe based porous ceramic Dew Point IEC system*

In operation, ambient hot, dry air is circulated through the dry channel transferring its heat to the heat pipes and part of which exists cool and dry while the other part of the air is redirected through the wet channel and in contact with the wet ceramic cuboids. Water contained in the ceramic cuboids seeps through the micro-pores in the cuboid's wall onto the outer surface to form a thin water film. Airflow around the ceramic containers in the wet channel causes continuous water evaporation from the cuboid's surface and subsequently cools the water inside the container, cooling the heat pipe condenser. The indirect pre-cooling of the air diverted into the wet channel provides additional potential to driving the evaporation process on the surface of the porous ceramic cuboids which effect is to attain higher temperature drop of supply air while rejecting spent working air at saturation conditions. The principle of operation of the heat pipe as a passive heat transfer device is not described in this work and can be found in many textbook [17]

3.2 Mathematical model

The mathematical model was formulated by applying heat, mass and momentum conservation equations of the airflows in the dry and wet channel. In addition, the ambient inlet air properties (dry bulb temperature, wet bulb temperature and moisture content) provide the initial conditions of the model while it was considered that there is no heat loss through the outer boundary. Similarly, the physical parameters of the system and properties of porous ceramic cuboids and heat pipes need to be defined as input parameters of the model. The specification of the heat pipes were provided by the manufacturer which include size, heat transfer limitations and material compatibility. Similarly, the porous ceramic cuboids' configuration, porosity and chemical composition were specified prior to manufacturing.

In this model, the dry and wet channel were divided into small finite volumes which embraces a heat pipe and the airflow properties were considered homogeneous, as shown in Fig. 7(a). The complex processes of heat and mass transfer in the dry and wet channel require the introduction of the following assumptions to simplify the model.

- *The air properties and local heat and mass transfer coefficients are constant.*
- *The mass of water vapour added to the airflow in the wet channel is small.*
- *Laminar air flow regime in both channels prevails.*
- *All outside boundaries are adiabatic.*
- *The air-water interface temperature is assumed equal to that of the water film temperature.*

A cross section of a single control volume of the computer model and associated input and output parameters is also shown in Fig. 7(b).

The cooling of the airflow in the dry channel is achieved through a series of convective and conductive heat transfer processes. This includes the convective thermal resistance at the interface between the airflow in the dry channel and the heat pipe wall and the airflow in the wet channel and the ceramic container surface, conductive thermal resistance through the wall of the heat pipe, its wick mesh, water layer in the container and the ceramic container wall. A simplified diagram of this network of thermal resistances connected in series is shown in Fig. 7 (a).

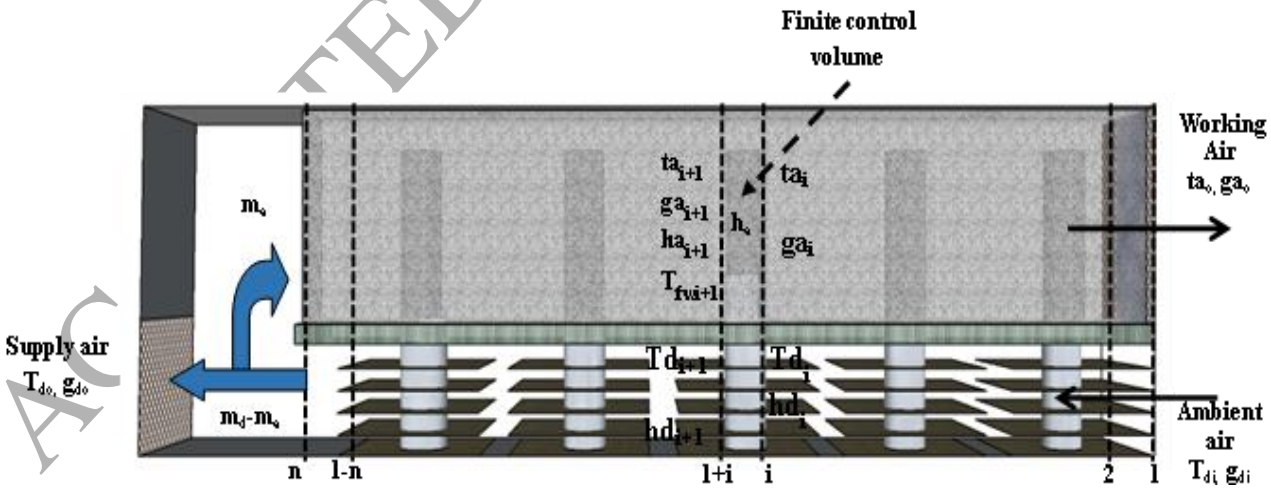

a)

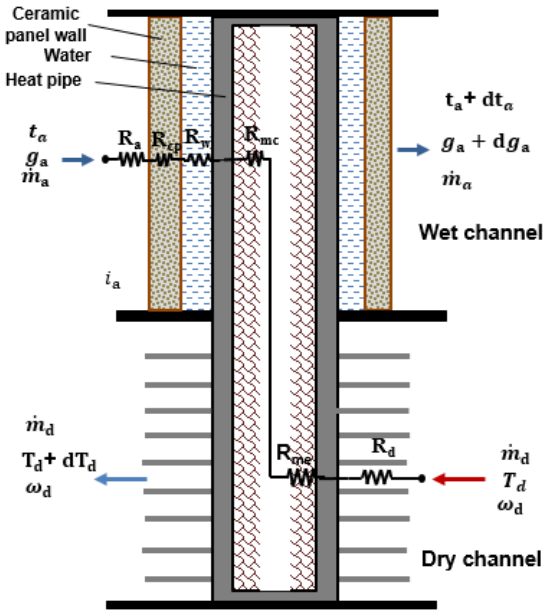

b)

Fig. 7. *a) Model control b) Single control volume lumped thermal resistance representation*

3.2.1 Overall heat transfer coefficient

The individual convective and conductive thermal resistances of each heat transfer process contributes to reducing heat flow between the airflow of the dry channel and wet channel. The equivalent thermal resistance can be expressed as:

$$R_T = \sum R_{th} = R_d + R_{me} + R_w + T_{cp} + R_o \quad (1)$$

where R_d is the convective heat transfer resistance of airflow over the finned heat pipe in the dry channel and is given as:

$$R_d = \frac{1}{\eta_f \alpha_d A_f} \quad (2)$$

Where, α_d is the convective heat transfer coefficient, A_f the area of the finned section of the heat pipe, and η_f is the efficiency of the fin which is expressed as [18]:

$$\eta_f = \frac{tan(hml)}{ml} \quad (3)$$

Where parameter $m = \left(\frac{2h}{\lambda_f \delta_f}\right)^{\frac{1}{2}}$ *is a function of the thickness of the fin,* δ_f *and its thermal conductivity,* λ_f.

The thermal resistance to heat flow in the heat pipe is primarily dominated by that of the wick through which the total heat crosses into and out of the vapour channel (heat supply at the evaporator and rejection at the condenser section). Therefore the thermal resistance of the copper tube wall (λ= 380 W/mK) and vapour channel are neglected in this analysis. This simplifies the thermal resistance of the tubular wick mesh to the following expression:

$$R_{me} = \frac{ln\left(\frac{r_2}{r_1}\right)}{2\pi\, l_1 \lambda_{wick}} \quad (4)$$

Where r_1 *and* r_2 *are the inner and outer radii of the circular wick mesh,* l_1 *is its length and* λ_{wick} *is the effective thermal conductivity of the wick material. The effective thermal conductivity of a saturated wick can be expressed as follows [15]:*

$$\lambda_{wick} = \frac{\lambda_l[\lambda_l+\lambda_s-(1-\varphi_{wick})(\lambda_l-\lambda_s)]}{\lambda_l+\lambda_s+(1-\varphi_{wick})(\lambda_l-\lambda_s)} \quad (5)$$

Where λ_l *and* λ_s *are thermal conductivity of the liquid phase of the working fluid of the heat pipe and thermal conductivity of wick material respectively and* φ_{wick} *is the wick porosity.*

The water layer between the heat pipe outer wall and the ceramic container inner wall is assumed to be static and the temperature of the water volume is uniform. The thickness of the water layer around the heat pipe was determined using the equivalent hydraulic diameter and the thermal resistance of the water layer can then be written as follows:

$$R_w = \frac{ln\left(\frac{r_w}{r_2}\right)}{2\pi\, l_w \lambda_w} \quad (6)$$

Where r_w *is the hydraulic radius of the rectangular water channel around the heat pipe,* l_w *is the height of the water in the container and* λ_w *is the water thermal conductivity.*

Similarly, the thermal resistance of the porous ceramic cuboid can be expressed as:

$$R_{cp} = \frac{d_{cp} A_{cp}}{\lambda_{cw}} \quad (7)$$

Where d_{cp} *is the wall thickness,* A_{cp} *is the heat transfer area and* λ_{cw}*is the effective thermal conductivity of the saturated ceramic wall which can rewritten from Equation (5) as:*

$$\lambda_{cp} = \frac{\lambda_w[\lambda_w+\lambda_c-(1-\varphi_c)(\lambda_w-\lambda_c)]}{\lambda_w+\lambda_c+(1-\varphi_c)(\lambda_w-\lambda_c)} \quad (8)$$

λ_c is the thermal conductivity of the dry ceramic container and φ_c is its porosity.

The convective thermal resistance between the airflow in the wet channel and the wet ceramic cuboid wall. Is expressed as follows:

$$R_a = \frac{1}{\alpha_a A_{cp}} \quad (9)$$

Where the evaluation of the heat transfer coefficients, α_a and α_d are dependents on the airflow properties and regime in the wet and dry channel respectively. Both airflow regimes are considered to be laminar and the heat transfer coefficient give as $\alpha = \frac{Nu\lambda_a}{L/N}$. The heat transfer coefficient is evaluated over a characteristic length equals that of the control volume (L/N) [19].

Finally, the overall heat transfer coefficient of the heat pipe-ceramic cuboid arrangement, K_s, can be expressed as a function of thermal resistance, as following:

$$K_s = \frac{1}{R_d+R_{me}+R_w+R_{cp}+R_a} = \left(\frac{1}{\alpha_d\eta_f A_f} + \frac{ln\left(\frac{r_2}{r_1}\right)}{2\pi\, l_1\lambda_{wick}} + \frac{ln\left(\frac{r_w}{r_2}\right)}{2\pi\, l_w\lambda_w} + \frac{d_{cp}A_{cp}}{\lambda_{cw}} + \frac{1}{\alpha_a A_{cp}}\right)^{-\frac{1}{2}}$$

(10)

3.2.2 Energy and mass conservation

The temperature and moisture content variation of the air in the dry and wet channels can be determined from the equation of heat and mass transfer conservation. In the dry channel, air is cooling by transferring its sensible heat to the heat pipe wall and fins at constant air moisture content. The heat is then transported and released as latent heat by the evaporation of water from the surface of the porous ceramic cuboid. This causes the temperature and moisture content of the airflow to increase along the wet channel, exiting at saturation conditions. The energy balance of a control volume in the dry channel can be expressed as follows:

$$\frac{\dot{m}_d c_{pd} dT_d}{dA} = -K_s\left(T_d - T_{wf}\right) \quad (11)$$

where, m_d is the air mass flow rate in the dry channel, C_{pd} is the specific heat of air, A is the heat transfer area, Ks is the overall heat transfer coefficient between the air flow in the dry and wet channel, T_d is the average temperature of air in a control volume in the dry channel, T_{wf} is the average

temperature of water film in control volume in the wet channel.

The heat transfer process in the wet channel is more complex. The airflow sensible heat is exchanged for latent heat of the water film on the surface of the porous ceramics. The energy balance in a control volume of the wet channel can be expressed as follows:

$$\frac{\dot{m}_a c_{pa} dt_a}{dA_a} = \alpha_a \left(T_{wf} - t_a\right) \quad (12)$$

Where, m_a is the air mass flow rate in the wet channel, α_a is the convective heat transfer coefficient between the wet surface and the airflow, A_a is the heat transfer area, t_a is the average temperature in the wet channel control volume, T_{wf} is the average temperature of water film of the control volume.

Similarly, the vapor mass transfer from the ceramic surface is driven by the vapour partial pressure difference. This can be expressed by the gradient in moisture content of the airflow and the water film as:

$$\frac{\dot{m}_a dg_a}{dA_a} = \sigma_a \left(g_{wf} - g_a\right) \quad (13)$$

Where, σ_a is the mass transfer coefficient, g_{wf} is the air moisture content at saturation, g_a is the average moisture content of air in the control volume. The relationship between heat and mass transfer coefficient in an evaporation process is usually given by Lewis number $= \frac{\alpha_a}{\sigma_a c_{pa}}$. in laminar flow regime, Lewis number falls within the range of 0.9 to 1.15 and to simplify the model it is usually assumed to be equal 1 [20].

To complete the mathematical model, the overall energy balance of the system is evaluated at the water film interface as follows:

$$\frac{\dot{m}_{wf} c_{pwf} dT_{wf}}{dA_a} = -K_s \left(T_d - T_{wf}\right) + \sigma_a \left(g_{wf} - g_a\right) + \alpha_a \left(T_{wf} - t_a\right) \quad (14)$$

3.2.3 Initial and boundary conditions

The computer model initial conditions include inlet ambient air temperature, relative humidity or moisture content) and mass flow rate. The branching out of part of the airflow at the outlet of the dry channel into the wet channel constitutes another boundary conditions in which the inlet air

temperature and moisture content of the wet channel are equal to those of the airflow at the outlet of the dry channel. It is also assumed that the outer boundaries of the cooling system are adiabatic.

3.3 Description of the experimental set-up

A small scale sub wet bulb evaporator was built to evaluate its performance and validate the computer model. The core component of the cooler is the HMX, which is made of two identical ceramic cuboid-heat pipes modules, each of which is made up of a porous ceramic cuboids of 360 x 220 x 42 mm and six tubular heat pipes. The ceramic cuboids and enclosed heat pipes condenser section are placed in the wet channel, whereas the heat pipes finned section (evaporator) occupies the dry channel. Fig. 8(a) shows the assembled laboratory prototype and Fig. 8(b) shows an example of a single module of a porous ceramic cuboid and three finned heat pipes. Looking in the direction of the wet channel airflow, a cross section down the middle of the cooling system is shown in Fig.8(c) which highlights the dry and wet channel with the direction of the airflow rate in each. In the dry channel, the air is draw in from a climatic chamber and flows through the fins of the heat pipes to maximise heat transfer. In the wet channel, however, the air flows through a front and back narrow gap formed between the outer casing of the cooler and the ceramic cuboids (Fig. 8c). The airflow over the wet surface of the ceramic cuboids causes water to evaporate, creating a temperature gradient potential across the heat pipe length.

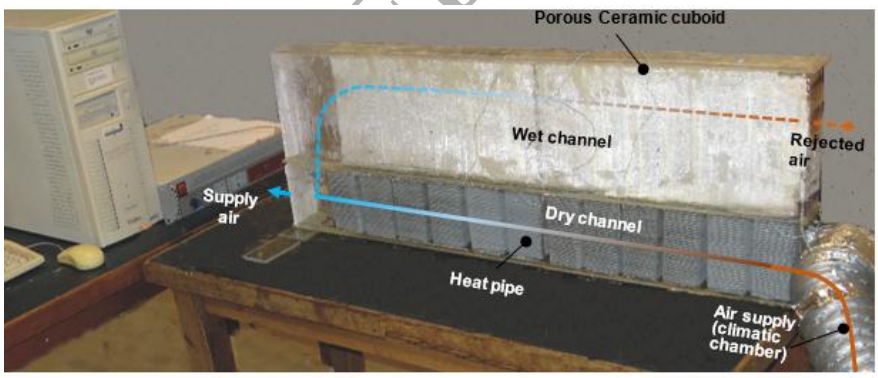

a)

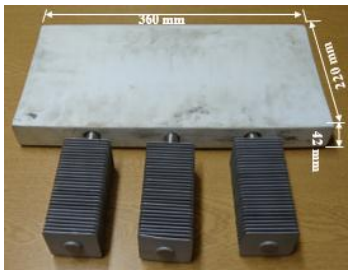

b)

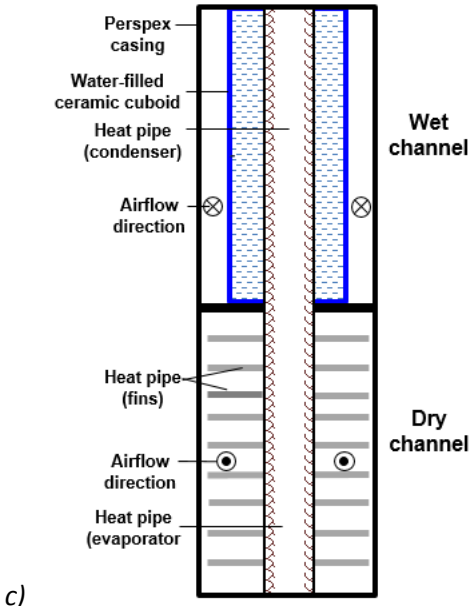

Fig. 8. *Laboratory test rig a) rig set up b) A heat pipe-porous ceramic cuboid module c) cross section of the cooler*

The main operating parameters of the cooler including inlet air temperature, relative humidity and mass flow rate were fully controlled. The inlet air was supplied from a climatic chamber with precision control of temperature and relative humidity while the mass air flow rate in both channels was controlled by changing the speed of a fan-motor and the opening and closing of the dry channel outlet damper grill. The main design and operating parameters of the rig are summarised in Table 1.

Table 1 *Main design and operating parameters*

Element	***Design and operating parameter***
Enclosure	
Material	*Clear Perspex*
Length x Width x Height	*820 x 380 x 52 mm*
Wall thickness	*5 mm*
Height of dry channel	*130 mm*
Height of wet channel	*220 mm*
Air inlet opening	*100 x 100 mm*
Supply air outlet opening	*100 x 100 mm*
Rejected air outlet opening	*100 x 100 mm*
Heat pipes	
Outer diameter	*18 mm*
Inner diameter	*15.8mm*
Mesh thickness (2 layers)	*0.16 mm*
Length of evaporator	*130 mm*
Length of condenser	*155 mm*
Length of adiabatic section	*10 mm*
Fluid	*de-ionised water*
Number of heat pipes	*12*
Porous Ceramic cuboids	
Materials compositions	Al_2O_3, $Si\ O_2$, *Albite, others*
Length	*360 mm*
height	*220 mm*
width	*42 mm*
Porosity	*19%*
Density	*2300 kg/m*^{3}
Thermal conductivity	*1.5 W/mK*

The test rig was fully instrumented and the main instruments used to measure temperature, relative humidity and airflow velocity are tabulated in Table 2.

Table 2 *Test rig instruments*

Measured parameter	*Instrument*	*Range*	*Accuracy of reading*
Air velocity	*Hotwire anemometer (Testo 405)*	*0 to 10 m/s*	*±5 %*
Relative Humidity / Temperature	*Humidity/temperature meter (RS-1361C)*	*10% - 95% RH*	*± 1% RH*
Air temperature	*Type K thermocouple*	*-50 to +250°C*	*±0.4%*
Water consumption	*Bench digital Scales (Kern FCB3K0.1)*	*0 to 3000g*	*±3%*
Dimensions	*Tape measure*	*0-1000mm*	*0.2%*
Data acquisition	*Data Taker (DT800)*	*-*	*-*

3.4 Experimental procedure

The dew point evaporative cooler prototype is connected to a climatic chamber via a flexible duct where the chamber is used to simulate the ambient conditions by setting and controlling air temperature and humidity. The hot, dry air supply is drawn in from the climatic chamber (Fig. 8a) at a flow rate controller by a variable-speed centrifugal fan. The supply air is cooled along the dry channel by transferring heat to the heat pipe finned evaporator while its moisture content remains unchanged. At the outlet of the dry channel, part of this cool supply air is diverted to the upper channel (wet channel) of the cooler to induce direct water evaporation from the porous ceramic cuboids and in the process removes heat transported by the heat pipe at its condenser. The warm and humid air at the wet channel at outlet is then rejected as spent air. The porous ceramic cuboids are continuously replenished with water from an overhead water tank. The thermal performance of the cooler was measured at inlet air temperatures from the climatic chamber of 30, 35 and 40 ^{o}C, relative humidity of 35, 40, 45, 50 and 55% and airflow speed of 0.5, 1 and 1.5 m/s.

4 Results

4.1 Airflow temperature profile in the air channels

The airflow temperature along the dry and wet channel was computed and experimentally measured, as shown in Fig. 9. The computer model predicted the air temperature to fall from 35 ^{o}C at the inlet to 21.98 ^{o}C at the outlet of the dry channel and increase again to 24.42 ^{o}C at the outlet of the wet channel. This was verified experimentally by placing five equidistant thermocouples at 0, 25%, 50%, 75% and 100% of the channel length and the measured outlet air temperature of the dry channel was 22.3 ^{o}C and that of the wet channel 25.01 ^{o}C, which represents a difference of 1.4 % and 11.0 % from computed results respectively. The discrepancy between the experimental and computer model results is larger in the wet channel because of the uneven airflow and water film distribution over the surface of the ceramic cuboids in the wet channel.

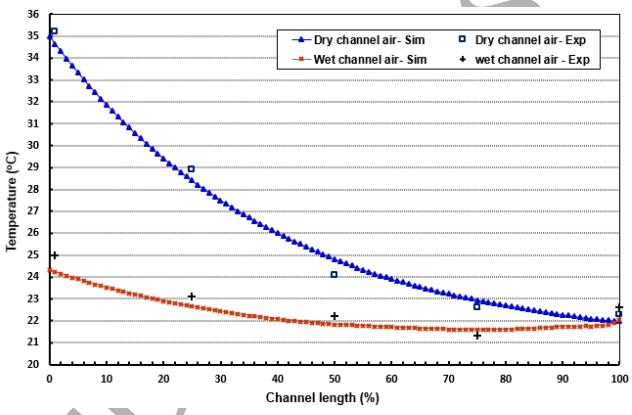

Fig. 9. *Air flow temperature profile in the wet and dry channel (T_{di}=35 ^{o}C and RH=35%)*

4.2 Psychometric operating conditions

Fig. 10 shows a psychrometric chart of the working properties of air in the cooler. The inlet air conditions are shown by the dry bulb temperature T_{di}= 35 ^{o}C and moisture content of approximately 12.3 (g/kg$_{d}$). The inlet air was cooled in the dry channel along a constant moisture content line from 35 ^{o}C to 22.3 ^{o}C, achieving sub wet bulb operating conditions (i.e., T_{wb}= 22.63 ^{o}C). The air rejected from the wet channel is fully saturated with a moisture content of 17.2 (g/kg$_{d}$).

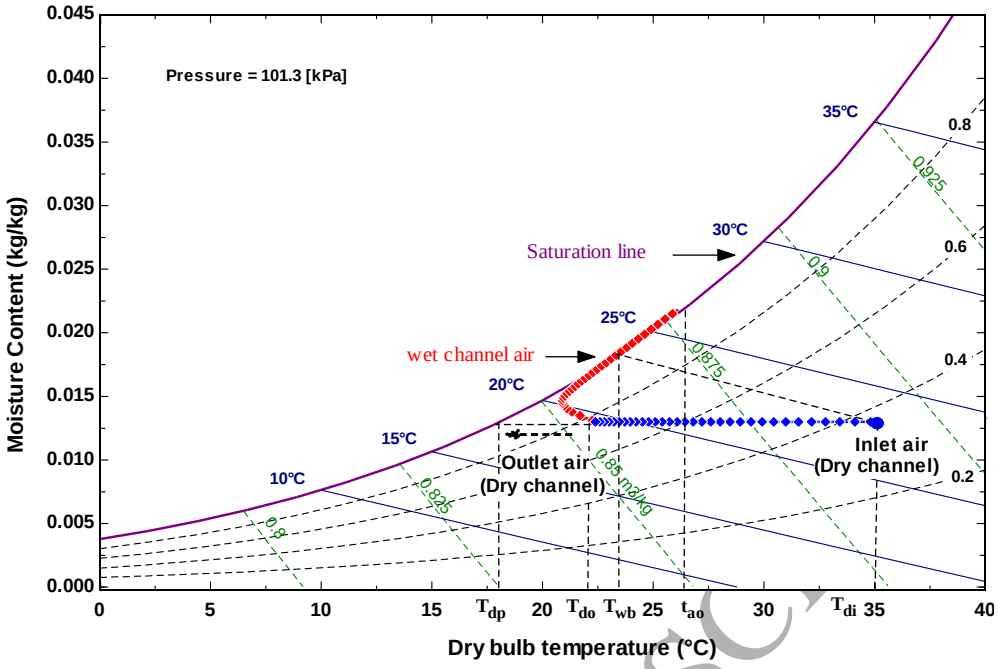

Fig. 10. *Psychrometric chart of air properties in the cooler*

4.3 Effect of inlet air temperature on cooling capacity

The cooling performance of the system is expressed per unit surface area of the wet porous ceramic area and is strongly dependent on the ambient air conditions. As the moisture content in the dry channel remains constant for a given inlet air relative humidity, the specific cooling capacity can be expressed as:

$$q_c = \frac{\dot{m}_s c_p}{A_a}(T_{di} - T_{do}) \qquad (15)$$

Fig. 11 shows both the effect of inlet air temperature and relative humidity on the system cooling capacity. It can be seen that the cooling capacity increases with increasing dry bulb temperature. For instance for a relative humidity of 35%, the computational model shows the cooling capacity increased from about 140 to over 270 W/m^2. Conversely, the cooling capacity decreases with increasing relative humidity. For inlet air dry bulb temperature of 35 ^{o}C the cooling capacity decreased from about 200 to 160 W/m^2 for relative humidity of 35 and 45% respectively These results are commensurate with observed performance trends of evaporative cooling technology. It can also be seen that there is good overall agreement between measured and computed results with maximum difference of less than 10%.

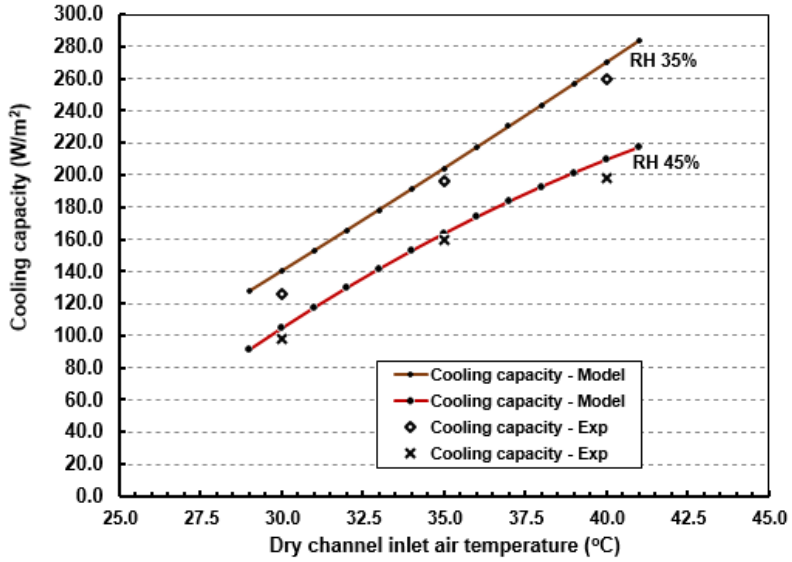

Fig. 11. *Effect of ambient air dry bulb temperature on cooling capacity*

4.4 Effect of relative humidity on cooling capacity and effectiveness

The effect of the ambient air relative humidity on cooling capacity of the system was further quantified analytically and experimentally as shown in Fig. 12. It can be observed that the cooling capacity decreases sharply with increasing relative humidity. The cooling effectiveness of the evaporative cooling system is expressed by the wet bulb and dew point effectiveness, ε_{wb} and ε_{dp} respectively, as follows:

$$\varepsilon_{wb} = \frac{T_{di} - T_{do}}{T_{di} - T_{wb}} \qquad (16)$$

$$\varepsilon_{dp} = \frac{T_{di} - T_{do}}{T_{di} - T_{dp,i}} \qquad (17)$$

Fig. 12 also shows that the variation in wet bulb and dew point effectiveness for relative humidity ranging from 35 to 55% and dry bulb temperature of 35 ^{o}C is small. The slight increase in dew point effectiveness of the system could appear confusing, as higher inlet air humidity should result in lower effectiveness of the cooler. This could simply be explained as for a given inlet temperature an increase in relative humidity leads to a decrease in its dew point, making the value of the denominator in the dew point effectiveness equation 17 small. The maximum wet bulb and dew point effectiveness was approximately 1.1 and 0.86 respectively.

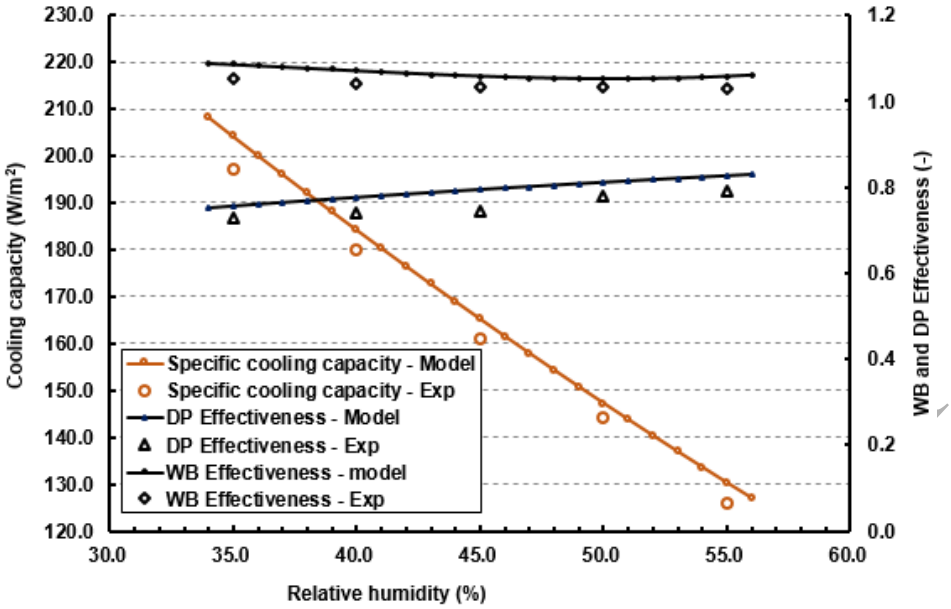

Fig. 12. *Effect of relative humidity on cooling capacity and effectiveness (T_{di}=35 ^{o}C)*

4.5 Effect of intake air velocity and relative humidity on water consumption

The effect of varying intake air velocity on water consumption was also modelled and measured. The operating conditions were considered for inlet air dry bulb temperatures of 35 ^{o}C, relative humidity of 35% and 55%, and velocity of 0.5, 1 and 1.5 m/s. Fig. 13 shows the water consumption trends for two levels of air relative humidity (35% and 55%) when air velocity was increased from 0.5 to 1.5 m/s. The step increase in water consumption is particularly attributed to increased rate of heat transfer between the air in the wet channel and the porous ceramic wet surface, leading to increased rate of water evaporation. At higher air velocities, part of the water consumption may also be caused by water droplets being entrained with the airflow. The model and experimental results are largely in good agreement with a maximum discrepancy of 10.9% occurred at high air flow velocity.

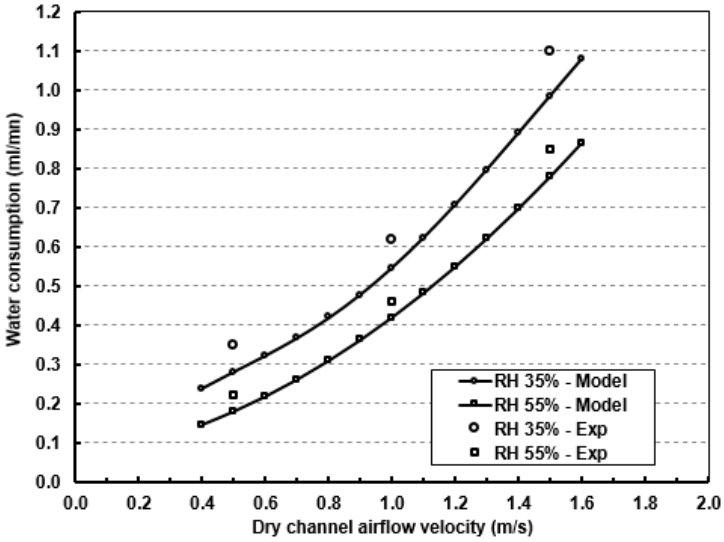

Fig. 13. *Effect of intake air channel velocity and relative humidity on water consumption (T_{di}=35 ^{o}C)*

4.6 Uncertainty analysis

The accuracy of computing the thermal performance of the evaporative cooling prototype (that is, cooling capacity and effectiveness) is subject to reading uncertainty associated with each instrument and sensor precision given in Table 2. The combined uncertainty of the specific cooling capacity of the system is determined as follows:

$$\boldsymbol{\delta q_c} = \sqrt{\left(\frac{\delta T_{do}}{T_{do}}\right)^2 + \left(\frac{\delta T_{di}}{T_{di}}\right)^2 + \left(\frac{\delta v_d}{v_d}\right)^2 + \left(\frac{\delta L}{L}\right)^2 + \left(\frac{\delta w}{w}\right)^2} \qquad (18)$$

Where δ_T is the relative uncertainty of the thermocouples temperature reading at the inlet and outlet of the dry channel, δv is the uncertainty of flow meter, δL and δw is the uncertainty of measuring the length and width of the porous ceramic cuboid wet area.

Similarly, the combined uncertainty of computing the evaporative cooling system effectiveness is determined from the uncertainty reading of the thermocouples of the dry bulb inlet and outlet temperature of the supply air as follows:

$$\boldsymbol{\delta\varepsilon} = \sqrt{\left(\frac{\delta T_{di}}{T_{di}}\right)^2 + 2\left(\frac{\delta T_{do}}{T_{do}}\right)^2} \qquad (19)$$

Using equation 18 and 19, the relative uncertainty of computing the cooling capacity and effectiveness of the cooling system from experimental measurements are presented in Table 3.

***Table 3**. The uncertainty of computed performance parameters*

Performance parameter	*Uncertainty (%)*
Cooling capacity	*± 5.04%*
Wet bulb effectiveness	*± 0.70%*
Dew point effectiveness	*± 0.70%*

Table 3 indicates that the maximum uncertainty of computing the cooling capacity of the system is around 5.04 % while the wet bulb and dew point effectiveness is 0.70%. The uncertainty analysis shows that the experimental results are subject to relatively small errors of measurements and provides a realistic assurance of the validity of the results.

5. Conclusion

A sub wet bulb evaporative cooling system consisting of water-filled porous ceramic cuboids and finned heat pipes was investigated theoretically and experimentally. A computer model was developed and an experimental test rig was constructed. The thermal performance of the system was evaluated under controlled laboratory conditions of airflow temperature, velocity and relative humidity.

The computational results were largely in good agreement with measured performance of the cooler. All the computer model results showed good match with measured performance trends of the system over the range of operating conditions. It was shown that the design could cool air below its wet bulb temperature and achieves wet bulb effectiveness above unity.

Furthermore, increasing inlet air temperature (T_{di}) led to an increase of cooling capacity while an increase of relative humidity reduced the cooling capacity sharply. In addition, the combined uncertainty of computed thermal performance indicators from measured parameters of the systems is relatively small.

The cooling performance of the system was evaluated as per unit of the porous cuboid external surface area. This is important in that the required cooling effect of an application can be related to a specific number of ceramic cuboids. The overall cost of the system depends largely on the number of ceramic cuboids and heat pipes. However, compared to other sub wet bulb temperature evaporative cooling designs where a PVC based compact HMX exchanger is used, the porous ceramic cuboid affords low maintenance cost, durability and flexibility to be produced in various shapes and sizes suitable for deploying as an integrated functional building element.

Acknowledgements

This paper wouldn't have been possible without the support of the following organizations:

- *General presidency for the affairs of holy mosque and the prophet's mosque.*
- *Majmaah University.*
- *The University of Nottingham.*

References

[1] A. Dodoo, L. Gustavsson, R. Sathre, Building energy-efficiency standards in a life cycle primary energy perspective, Energy Build. 43 (7) (2011) 1589–1597.

[2] L. Pérez-Lombard, J. Ortiz, F. Juan, J.F. Coronel, I.R. Maestre, A review of HVAC systems requirements in building energy regulations, Energy Build. 43 (2–3) (2011) 255–268.

[3] D.R. Vissers, Study on building integrated evaporative cooling of glass-covered spaces, in: Building Physics and Systems, Eindhoven University of Technology, 2011.

[4] G.J. Bom, E.R.F. Dijkstra, M. Tummers, Evaporative Air-Conditioning Applications for Environmentally, The Word Bank, Washington, DC, 1999.

[5] A. Alharbi, R. Boukhanouf, T. Habeebullah, H. Ibrahim, Thermal performance and environmental assessment of evaporative cooling systems: case of Mina Valley, Saudi Arabia, Int. J. Civil, Arch. Struct. Constr. Eng. 8 (5) (2014) 539– 5443.

[6] T. Gunhan; V. Demir; A.K. Yagcioglu, Evaluation of the Suitability of Some Local Materials as Cooling Pads, Biosystems Engineering (2007) 96 (3), 369–377.

[7] M. Barzegar, M. Layeghi, G. Ebrahimi, Y. Hamzeh , M. Khorasani, Experimental evaluation of the performances of cellulosic pads made out of Kraft and NSSC corrugated papers as evaporative media, Energy Conversion and Management 54 (2012) 24–29.

[8] B. Riangvilaikul, S. Kumar, Numerical study of a novel dew point evaporative cooling system, Energy and Buildings 42 (2010) 2241–2250.

[9] B. Riangvilaikul, and S. Kumar, An experimental study of a novel dew point evaporative cooling system. Energy and Buildings, 42(5) (2010) pp. 637-644.

[10] X. Zhao, S. Yang, Z. Duan and S. B. Riffat., Feasibility study of a novel dew point air conditioning system for China building application. Building and Environment,. 44(9) (2009) pp. 1990-1999.

[11] C. Zhan, X. Zhao, S. Smith and S.B. Riffat, Numerical study of a M-cycle cross-flow heat exchanger for indirect evaporative cooling. Building and Environment, 46(3) (2011) pp. 657-668.

[12] E. Ibrahim, L. Shao and S. B. Riffat, Performance of porous ceramic evaporators for building cooling application, Energy and Buildings 35 (2003) 941–949.

[13] W. Chen, Song Liu, Jun Lin, Analysis on the passive evaporative cooling wall constructed of porous ceramic pipes with water sucking ability, Energy and Buildings 86 (2015) 541–549.

[14] F. Wang, T. Sun, X. Huang, Y. Chen and H. Yang, Experimental research on a novel porous ceramic tube type indirect evaporative cooler, Applied Thermal Engineering, Volume 125, 2017, Pages 1191-1199.

[15] S. B. Riffat and J. Zhu, Mathematical model of indirect evaporative cooler using porous ceramic and heat pipe. Applied Thermal Engineering, 2004. 24(4): p. 457-470.

[16] R. Boukhanouf, O. Amer, H. Ibrahim and J. Calautit, Design and performance analysis of a regenerative evaporative cooler for cooling of buildings in arid climates, Building and Environment, 142 (2018).

[17] D. Reay, R. McGlen and P. Kew (2013). Heat Pipes Theory, Design and Applications. 6th Edition. Butterworth-Heinemann.

[18] B. Halasz, A general mathematical model of evaporative cooling devices. Elsevier, Paris, 1998: p. 245-255.

[19] R. K. Shah and D. P. Sekulic, Fundamentals of heat exchanger design. 2003, Canada: Jon Wiley& Sons.

[20] W.P. Jones, Air Conditioning Engineering, 5th Edition, Butterworth Heinemann (2001).